Neutron irradiation defects in gallium sulfide: Optical absorption measurements

F. J. Manjón, A. Segura, and V. Muñoz
Departamento de Física Aplicada (Facultad de Física) e Instituto de Ciencia de Materiales de la Universidad de Valencia (ICMUV), C/. Dr. Moliner, 50 Ed. Investigación: 1-014 E-46100 Burjassot, Valencia, Spain

(Received 2 January 1997; accepted for publication 31 January 1997)

Gallium sulfide single crystals have been irradiated with different thermal neutron doses. Defects introduced by neutron irradiation turn out to be optically active, giving rise to absorption bands with energies ranging from 1.2 to 3.2 eV. Bands lying in the band-gap exhibit Gaussian shape. Their energies and widths are independent of the irradiation dose, but their intensities are proportional to it. Thermal annealing is completed in two stages, ending at around 500 and 720 K, respectively. Centers responsible for the absorption bands are proposed to be gallium-vacancy-gallium-interstitial complexes in which the distance between the vacancy (acceptor) and the interstitial (donor) determines the energy and intensity of the absorption band, as well as the annealing temperature. © *1997 American Institute of Physics.* [S0021-8979(97)00610-5]

I. INTRODUCTION

Gallium sulfide (GaS) is one of the less studied compounds of the III–VI family, which also includes gallium and indium selenides (GaSe,InSe). GaS is a layered material with a crystal structure that consists of graphitelike layers bound by Van der Waals forces, unlike the forces inside the layers which are of covalent type. GaS is a semiconductor with an indirect energy gap of 2.5 eV at room temperature and has been proposed as a promising material for near-blue-light-emitting devices.[1]

Heavy concentrations of impurities in III–VI laminar compounds are difficult to obtain by conventional doping methods due to the high degree of impurity segregation in such structures;[2] however, attempts to use neutron transmutation doping (NTD) have been successful in increasing the dopant concentration on others III–VI semiconductors.[3,4] In NTD the sample is exposed to thermal neutron irradiation. Some isotopes from the chemical species in the sample transmute into other ones by neutron capture and subsequent β decay. This doping technique has two main advantages:

(i) the amount of impurities can be properly controlled if the flux of thermal neutrons and the neutron capture cross sections are known; and
(ii) the distribution of impurities is uniform provided that isotopes are homogeneously distributed in the material.

The drawback is that transmuted atoms are likely to be displaced out of their original positions because of the γ and β recoils involved in the transmutation processes. Thus a great number of defects results from these recoils and the residual flux of epithermal neutrons. In order to remove lattice damage and electrically activate the transmuted impurity atoms, thermal annealing at high temperatures is required.

Defects due to neutron irradiation in GaS turn out to be optically active. In this work we study the thermal annealing of neutron irradiated GaS through optical absorption measurements. Experimental details are presented in Sec. II, where a description of the doping and thermal annealing processes is given. The results on the optical properties of the material due to irradiation defects as a function of neutron dose and temperature are presented in Sec. III. And finally, in Sec. IV, we present a defect model based in close vacancy-interstitial complexes which is shown to be coherent with most results here reported.

II. THEORETICAL AND EXPERIMENTAL DETAILS

A. Neutron capture and radiation damage in GaS

The host atoms of GaS mainly consist of two Ga isotopes and two S isotopes. Gallium isotopes are $^{69}_{31}$Ga and $^{71}_{31}$Ga whose natural abundancies are 60.1% and 39.9%, respectively. On the other hand, sulfur isotopes are $^{32}_{16}$S, which accounts for 95.02%, and $^{34}_{16}$S in a proportion of 4.21%. Other isotopes of sulfur are in negligible concentrations.[5]

When GaS is exposed to thermal neutrons the main reactions are those concerning Ga isotopes,

$$^{69}_{31}\mathrm{Ga}+n \xrightarrow{\sigma=1.7b} {}^{70}_{31}\mathrm{Ga}+\gamma, \quad E_\gamma=7 \text{ MeV},$$

$$^{70}_{31}\mathrm{Ga} \xrightarrow{\tau=21.1 \text{ min}} {}^{70}_{32}\mathrm{Ge}+\beta^-, \quad E_{\beta^-}=1.653 \text{ MeV},$$

$$^{71}_{31}\mathrm{Ga}+n \xrightarrow{\sigma=4.7b} {}^{72}_{31}\mathrm{Ga}+\gamma, \quad E_\gamma \cong 6.5 \text{ MeV},$$

$$^{72}_{31}\mathrm{Ga} \xrightarrow{\tau=13.95 \text{ h}} {}^{72}_{32}\mathrm{Ge}+\beta^-, \quad E_{\beta^-}=3.15 \text{ MeV},$$

where σ is the neutron capture cross section and τ is the β-decay lifetime.

An estimation of the extrinsic impurities in GaS irradiated samples can be made by using the equation[6]

$$n_{\mathrm{NTD}}=\Phi \sum_i n_i \sigma_i, \tag{1}$$

where n_i is the concentration of isotope i, σ_i its thermal neutron capture cross section, and i extends over all isotopes

in sample. $\Phi=\phi t$ is the thermal neutron fluence given by the product of thermal neutron flux ϕ and the time of exposition of sample t.

In the above-described reactions, resulting nuclei are not usually in their original positions but displaced into interstitial positions due to atom recoil resulting from momentum conservation in γ and β decays. Fast neutron knock-on can also give rise to atom displacement. The recoil energies from γ and β emissions are

$$E_R(\gamma)=E_\gamma^2/2Mc^2, \tag{2}$$

$$E_R(\beta)=E_\beta(E_\beta+2mc^2)/2Mc^2, \tag{3}$$

where M is the mass of the recoiling nucleus, m is the electron rest mass, and E_γ and E_β are the energies of γ and β particles, respectively. Recoil energies due to γ emission cover a range of values because various decay channels are possible. On the other hand, recoil energies associated with β decay show a continous spectrum because they depend on the correlation between the emitted neutrino and the β particle.

Energies of only 10–20 eV are required for the creation of Frenkel defects in semiconductors [9–10 eV in GaAs,[6] 10–20 eV in Si (Ref. 7)]. These energies are by far much lower than those released in γ and β reactions. The atom energy recoils in GaS according to Eqs. (2) and (3) range from 30 to 400 eV; therefore, a great number of defects is expected in samples due to neutron irradiation.

B. Experimental setup

The GaS monocrystals used in this study have been grown by the Bridgman–Stockbarger method from a stoichiometric polycrystalline melt obtained by diffusion of sulfur over melt gallium. The nominal purity of constituent elements (gallium and sulfur) was of 6N. Slabs about 1 mm thick and $5\times10\ \mathrm{mm}^2$ in size were cleaved from the ingot and exposed to a thermal neutron flux of $4.4\times10^{11}\ \mathrm{n/cm^2\ s}$, during 35, 70, 138, and 253 h, in order to get fluences between 5×10^{16} and $4\times10^{17}\ \mathrm{n/cm^2}$. We refer to these slabs as F1, F2, F3, and F4, respectively. During irradiation, the fast neutron flux on the samples was lower than 5% of the thermal neutron flux and the sample temperature was 303 K. In these conditions, according to Eqs. (1), (2), and (3), and taking into account GaS parameters, the estimated Ge concentration in samples irradiated for 253 h is about $2.7\times10^{16}\ \mathrm{cm^{-3}}$, which is a much lower concentration than the defect concentration that is expected from atom recoil mechanisms.

Samples for optical measurements, with thicknesses ranging from 5 to 250 μm, were cleaved from irradiated slabs. The absorption coefficient of samples from all irradiated slabs and a reference nonirradiated sample was measured at room temperature. Isochronal annealing at temperatures up to 800 K was performed only for samples from the F4 slab. At each annealing step samples were heated in vacuum (10^{-3} mbar) for 10 min, in a furnace specially designed to carry out *in situ* optical measurements.[4]

The optical setup consists of a halogen lamp as light source, a focusing mirror, a mechanical chopper, an H25 Jobin–Yvon monocromator with a 25 cm focal, the annealing furnace (with focusing lenses for the incoming and outcoming beams), and a Si or Ge photodiode whose signal was measured with a lock-in amplifier and stored in a computer.

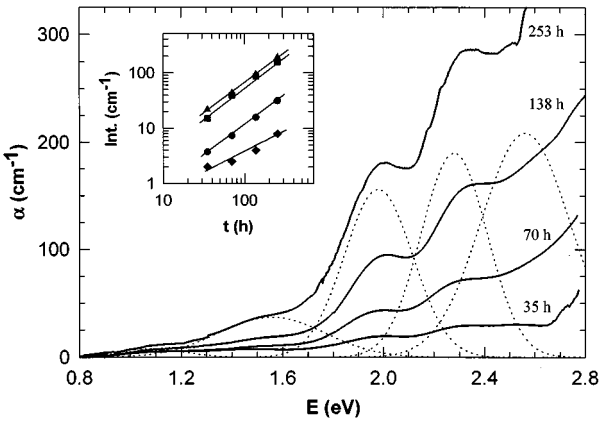

FIG. 1. Extrinsic absorption coefficient of NTD GaS at RT vs photon energy for several exposition times of samples to neutron irradiation: 35 h; 70 h; 138 h; 253 h. Inset: Intensity of the absorption bands obtained from Gaussian fits vs the neutron exposition time: (♦) B1; (●) B2; (■) B3; (▲) B4.

The furnace sample holder has three holes: one for the irradiated sample, another for a nonirradiated reference sample with the same thickness, and the other for the direct beam. The absorption coefficient was measured from the experimental transmittancy,[8] $T=I/I_0$ by the sample-in–sample-out method: I is the intensity transmitted through the sample and I_0 the direct beam intensity. Below the absorption edge of each sample a constant transmittancy is attained, which is scaled by a constant factor so as to give the theoretical value of a transparent semiconductor slab, which is given by $T_0=(1-R)^2/(1-R^2)$. The absorption coefficient is then determined from the scaled transmittancy through

$$\alpha=\frac{1}{d}\ln\left\{\frac{(1-R)^2}{2T}+\left[\left(\frac{(1-R)^2}{2T}\right)^2+R^2\right]^{1/2}\right\}, \tag{4}$$

where R is the reflectivity of the sample, which is a function of the refractive index n. The refractive index of GaS has been taken by extrapolation from data of McMath and Irwin.[9]

In all spectra shown in the figures of Sec. III the GaS intrinsic absorption has been subtracted. They correspond to the absorption contribution of irradiation defects.

III. RESULTS

A. Optical absorption coefficient as a function of neutron fluence

Figure 1 shows the extrinsic absorption coefficient of all irradiated slabs in the spectral range from 0.8 to 2.8 eV at room temperature (RT). The enhancement of the absorption with increasing the neutron fluence clearly appears. Below the GaS intrinsic absorption edge, bands at energies of 1.2 (B1), 1.55 (B2), 1.97 (B3), and 2.28 eV (B4) are observed.

Bands B1, B2, B3, and B4 have Gaussian shape and their energies and widths are independent of the neutron

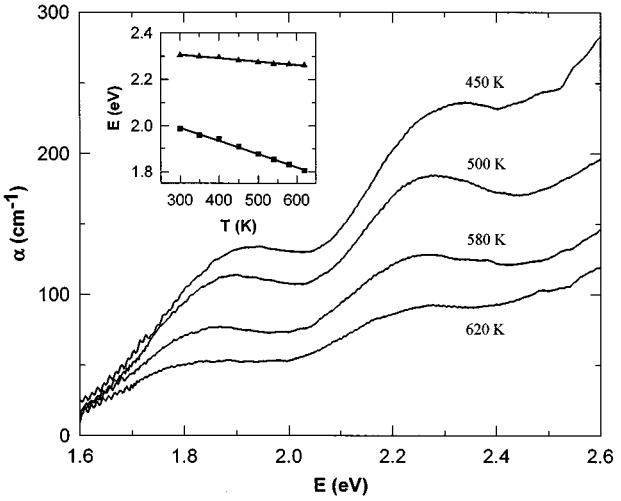

FIG. 2. Extrinsic absorption spectra of NTD GaS at the annealing temperature between 450 and 620 K. Inset: Photon energy of the absorption bands as a function of temperature: (■) B3; (▲) B4.

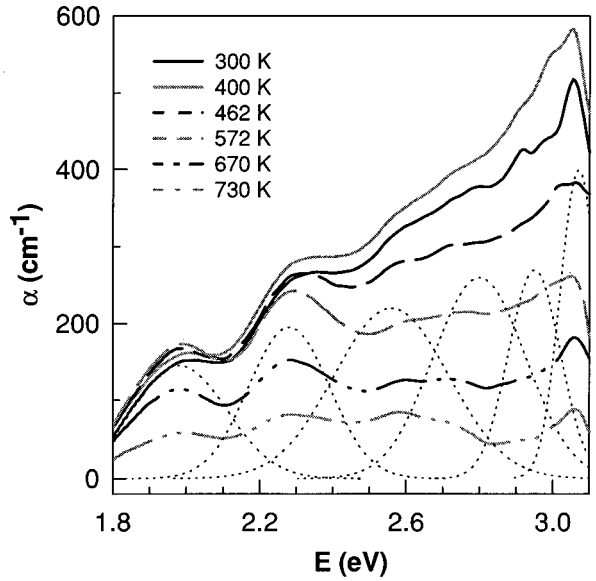

FIG. 3. Absorption spectra of NTD GaS at RT after annealings at temperatures between 300 and 730 K.

dose. Their intensities are proportional to the irradiation time, and therefore to the neutron fluence, as shown in the inset of Fig. 1. No saturation effects are observed in the explored neutron fluence range. A decomposition of the absorption spectrum of slab F4 in several Gaussians is shown in Fig. 1.

Extrinsic absorption is also observed for photon energies higher than the GaS indirect gap, suggesting the presence of resonant levels associated to irradiation defects. A band at 2.56 eV (R1) is also shown in Fig. 1. (These bands appear more clearly in Fig. 3 in which the spectral range is extended up to 3.1 eV.) This part of the extrinsic absorption can also be decomposed in several Gaussian bands at energies 2.56 (R1), 2.80 (R2), 2.95 (R3), and 3.07 eV (R4) (as shown in Fig. 3).

B. Optical absorption coefficient at the annealing temperature

The absorption coefficient was measured at the annealing temperature in order to compare the temperature shift of the band energies with that of the GaS indirect gap. Figure 2 shows the extrinsic absorption spectrum of samples from the F4 slab at the annealing temperature. Bands shift to lower energies with increasing temperature, but they conserve the Gaussian shape. The energy shift is linear in the explored temperature range, as illustrated in the inset of Fig. 2. The temperature coefficients are -0.45, -0.58, and -0.15 meV/K for bands B2, B3, and B4, respectively. The bandwidths also increase with temperature. The behavior of the absorption intensity at the annealing temperature is not discussed here, as it is determined by two different mechanisms that cannot be distinguished in that temperature range: the temperature effect on the absorption center parameters and the temperature effect on the defect concentration (defect recombination). Optical absorption measurements at low temperature would be necessary to isolate the first mechanism.

C. Optical absorption coefficient at room temperature after annealing

Figures 3 and 4 show the extrinsic absorption coefficient of samples from slab F4 at RT, after annealings at temperatures between 300 and 730 K. In the absorption coefficient range shown in Fig. 3, only bands B3 and B4 are well resolved. Figure 4 corresponds to a lower absorption range, where bands B1, B2, B3, and B4 are observable. After each annealing step, absorption bands conserve the Gaussian shape. Their energies and widths at RT do not change considerably after annealing at higher temperatures.

As regards their intensities after annealing, they exhibit different behaviors that can be qualitatively described from the spectra shown in Figs. 3 and 4. Resonant bands have a maximum intensity at 400 K, and begin to disappear above this temperature. Band B2 is no longer observable above 500 K. Regarding bands B1, B3, and B4, their intensities slightly increase up to 500 K and then steply decrease between 550 and 700 K. This suggests that the defect recombination process is achieved in two steps. Figure 5, which shows the temperature dependence of the integrated intensity of the extrinsic absorption for different spectral ranges, confirms this hypothesis. All plots in Fig. 5 have an inflexion between 450 and 550 K, and the integrated intensity tends to vanish above 700 K.

Figure 6 shows the Arrhenius plot of the intensity of bands B3 and B4 and that of the integrated absorption of resonant bands. Fits calculated according to kinetics models, and shown as solid lines in Fig. 6, are discussed in Sec. IV. Let us now point out that these Arrhenius plots show that the centers responsible for resonant bands start recombining at a lower temperature and with a lower activation energy than those responsible for bands in the band gap.

It must be outlined that, after annealing at temperatures above 750 K, all samples exhibit oxide layers whose interferencial effect on the transmittancy spectra is stronger than

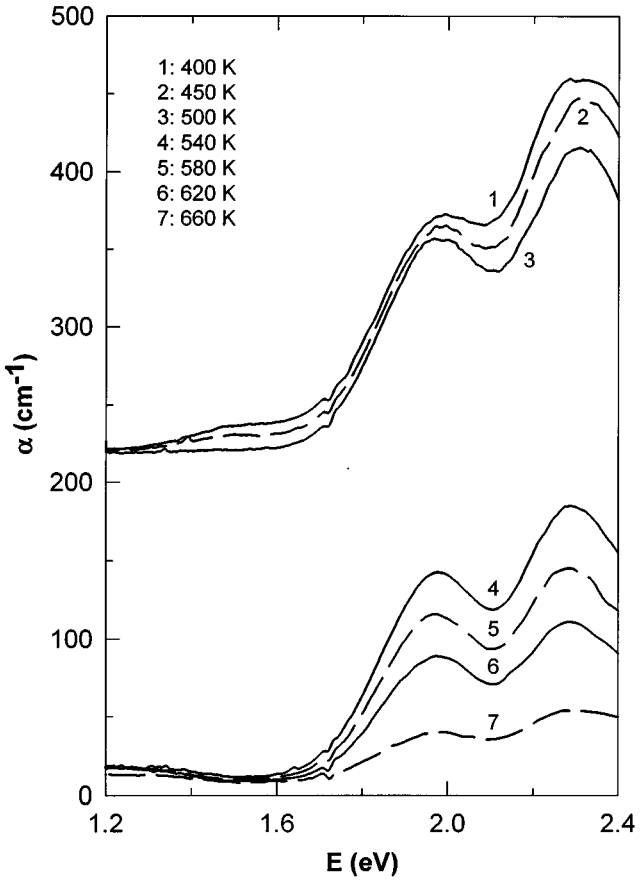

FIG. 4. Absorption spectra of NTD GaS at RT in the photon energy range between 1.2 and 2.4 eV, after annealings at different temperatures. Curves 1–3 are shifted by 200 cm^{-1}.

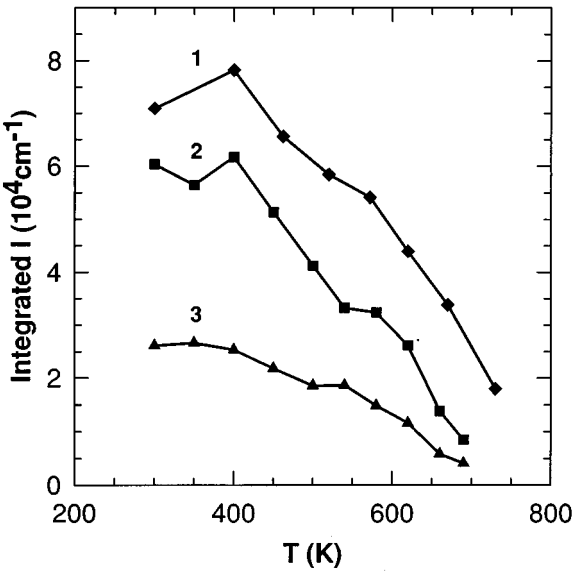

FIG. 5. Integrated intensity of absorption bands at RT for several photon energy ranges vs the annealing temperature. Curve 1:1.6–3.1 eV; curve 2:1.6–2.5 eV; curve 3:1.2–2.0 eV.

that of the absorption of not recombined irradiation defects. As a result, the extrinsic absorption coefficient could not be accurately determined above that temperature. Nevertheless, after annealing at 800 K, and once the oxidized surface layers are cleaved samples do not exhibit any extrinsic absorption, which means that the Ge transmuted atoms do not modify the GaS intrinsic absorption edge.

IV. DISCUSSION

From studies made on neutron-irradiated materials,[10] it is known that the irradiation defects are homogeneously distributed and mainly consist of vacancy-interstitial pairs. It seems reasonable to assume that in GaS most of these pairs are Ga vacancy-interstitial pairs; at first, because Ga atoms are those primarily removed by recoil in β and γ decays, and also because, the Ga atomic number being higher, Ga atoms interact more strongly with all sources of secondary displacements (Ga recoiled atoms, β and γ rays).

In order to propose a model coherent with results reported in Sec. III, we point out some features of the extrinsic absorption in NTD-GaS:

(i) Absorption bands have Gaussian shape; this fact, along with the temperature dependence of their energy and width, is typical of complex centers, formed by close donor–acceptor pairs;

(ii) the absorption band energies cover an interval from 1.2 eV (band B1) to 3.2 eV (resonant bands);

(iii) the band absorption intensity is correlated with its energy position: Higher-energy bands have higher absorption intensity; and

(iv) defects responsible for resonant bands start recombining at a lower temperature than that of centers responsible for bands B1, B3, and B4.

On the assumption that most displaced atoms are the Ga ones, the complex centers responsible for the absorption bands would be formed by a Ga vacancy (with acceptor character) and a Ga interstitial (with donor character), at different

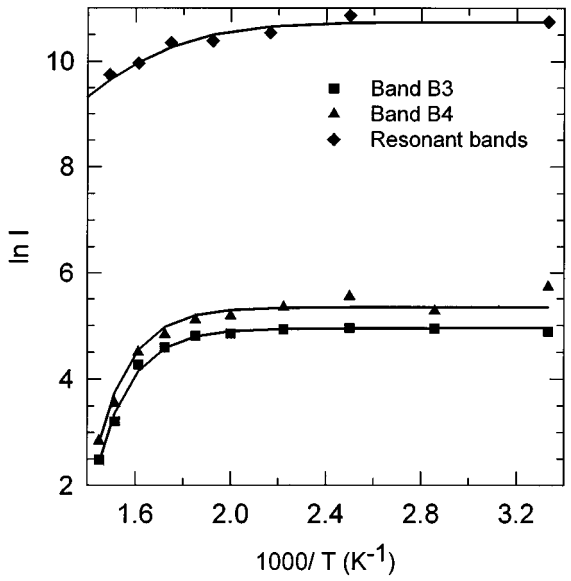

FIG. 6. Arrhenius plot of the integrated intensity at RT of bands B3 and B4 and resonant bands vs the inverse of the annealing temperature.

distances. The vacancy-interstitial distance would determine the photon energy and intensity of the optical transition as well as the annealing temperature.

Let us at first discuss the annealing temperature and recombination kinetics. The annealing kinetics of two types of defects that are homogeneously distributed and recombine with each other is given by a second-order reaction.[11] Taking into account that isochronal annealing is given to samples, we can obtain the impurity concentration as a function of temperature. Assuming that the intensities of the induced absorption bands are proportional to the defect concentration, we have

$$I=\frac{I_0}{1+BT^2\,\exp(-E_a/kT)}. \tag{5}$$

This equation can be fitted to the Arrhenius plot of resonant bands (Fig. 6) yielding an activation energy of 0.3 eV, which corresponds to an annealing temperature of 500 K, but not to that of bands B3 and B4. In fact, centers responsible for these bands seem to recombine through a first-order reaction, which, when isochronal annealing is taken into account, leads to the following equation:

$$I=I_0\,\exp\left[-CT^2\,\exp\left(-\frac{E_a}{kT}\right)\right]. \tag{6}$$

Fitting Eq. (6) to the Arrhenius plot of bands B3 and B4 yields an activation energy of 0.5 eV, corresponding to an annealing temperature of 650 K. This activation energy would be a migration energy of vacancies or interstitial atoms, which corresponds to a first-order process.

Investigations on neutron-irradiated InSe (Ref. 4) show that the recovery of recoil-induced damage is accomplished in two stages. The recovery at temperatures between 325 and 375 K is attributed to close pairs recombination, while the recovery at temperatures above 375 K is attributed to the annealing of isolated centers V_{In} and/or V_{In}–$\mathrm{Sn}_{\mathrm{In}}$ nonclose pairs. Results here reported indicate a similar behavior in GaS: During neutron irradiation recoiling atoms create a high concentration of Ga vacancies and interstitials at different distances. Only pairs at distances not much higher than the sum of the effective donor and acceptor Bohr radius can contribute to extrinsic absorption. In the first annealing steps, as displaced atoms become mobile the formation of donor–acceptor pairs is enhanced. This explains the fact that between 300 and 400 K the intensity of all bands increases. Above 400 K close vacancy-interstitial pairs start recombining in a second-order reaction (the intensity of resonant bands starts decreasing). At higher temperatures nonclose pairs become close pairs by vacancy or interstitial migration (first-order process). This would correspond to the decrease of intensities of bands B3 and B4 and explains also why resonant bands are still observed at that temperature.

This model is coherent with the photon energy range at which the different bands are observed. The optical transition between the ground (acceptor) and the excited (donor) states is expected to occur at a photon energy given by

$$\hbar\omega_{\mathrm{AD}}=E_G-E_D-E_A+\frac{e^2}{4\pi\epsilon R}, \tag{7}$$

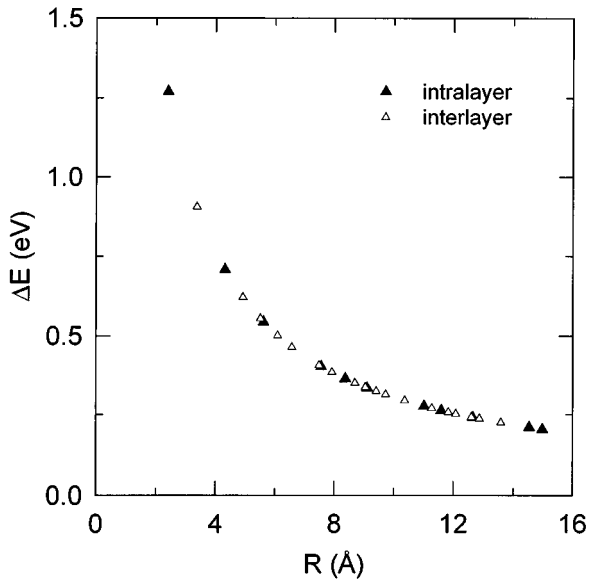

FIG. 7. Coulombian repulsion at a donor–acceptor pair according to the third term of Eq. (7) Solid symbols: interstitials located in intralayer sites; empty symbols: interstitials located in interlayer sites.

where E_G is the band-gap energy, E_D and E_A are the ionization energies of the donor and the acceptor centers, R is the donor–acceptor distance, and ϵ is the static dielectric constant of the material. The fourth term in the right-hand part of Eq. (7) corresponds to the Coulombian repulsion between the hole in the acceptor and the ionized donor. If the acceptor is a Ga vacancy, this repulsion energy can be calculated for the most likely positions of the interstitial (the hexagonal intralayer site and the octahedral interlayer site) at different distances from the vacancy. Figure 7 shows the results of that calculation, using ϵ_∞ instead of ϵ_0, which is justified by the very localized character of donor and acceptor states in GaS.[12] The photon energy range in which extrinsic absorption bands are observed is of the order of 1.8 eV. The repulsion energy for the shortest vacancy-interstitial distance is of the order of 1.3 eV. This can be considered as a good agreement given the simplifying assumptions involved in Eq. (7). From this equation a vacancy-interstitial distance can be estimated for each center on the assumption that the lowest photon energy at which bands are observed corresponds to $E_G-E_D-E_A$.

On the other hand, the relative intensity of the absorption bands of complex centers formed by donor–acceptor pairs depends on the vacancy-interstitial distance. The photon absorption by a donor–acceptor pair corresponds to the transition from the acceptor level to the donor level. The intensity of this transition would depend on the dipolar matrix element. On the assumption of both states being described by hydrogenic s functions and the electric field of the incident light being oriented parallel to R, the dipolar matrix element would be given by

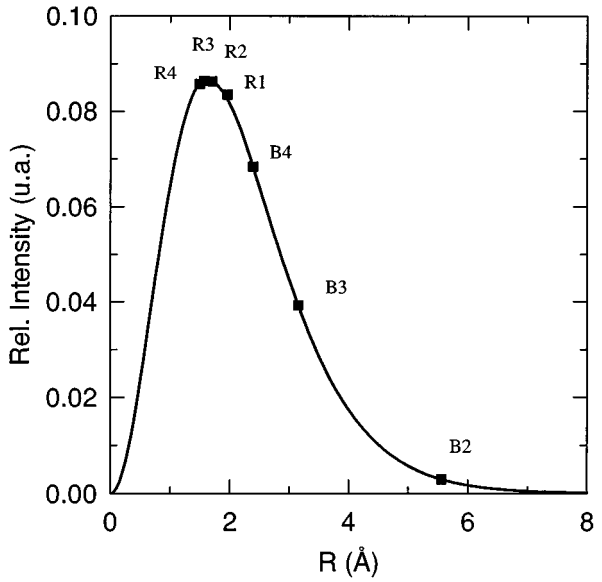

FIG. 8. Solid line: Relative intensity of electronic dipolar transitions from the ground to the excited level in the complex center vs the acceptor–donor distance as calculated from Eq. (8) with $C=1$, $r_a=0.5$ Å, and $r_d=1.5$ Å. Symbols correspond to the relative intensities at donor–acceptor distances calculated from Eq. (7) for each band.

$$M_{\mathrm{vc}}=\langle \Psi_v|z|\Psi_c\rangle$$

$$=C\int e^{-r'/r_d}\, r\, \cos\,\theta e^{-r/r_a}\, r^2\, \mathrm{sen}\,\theta\, d\theta\, dr, \qquad (8)$$

$$r'=\sqrt{r^2+R^2-2rR\,\cos\,\theta},$$

where C is a proportionality constant, r_a is the acceptor radius, r_d is the donor radius, R is the acceptor–donor distance, and θ the angle formed by the radius vector r and the direction of the electric field of the incident light (z axis). For a homogeneous defect concentration one can assume that pairs at different distances are in very similar concentrations. Therefore, the absorption coefficient would be proportional to the square of the matrix element. Figure 8 shows the square of the matrix element versus the donor–acceptor distance as calculated from Eq. (8) with $r_a=0.5$ Å and $r_d=1.5$ Å. Symbols in Fig. 8 indicate the calculated relative intensities corresponding to the distances associated to each band through Eq. (7). Those intensities are in qualitative agreement with those experimentally observed.

It must be outlined that only band B2 exhibits a behavior not explained by this model. Two interpretations can be invoked:

(i) Band B2 is related to very close donor–acceptor pairs in which an attractive term due to Van der Waals interaction compensates the repulsion term in Eq. (7),[13,14] this would be coherent with the fact that band B2 is no longer observable above 500 K;

(ii) band B2 could be related to centers not included in the model such as bivacancies or sulfur vacancies or interstitials.

V. CONCLUSIONS

Results on optical absorption centers induced by the NTD method in GaS show that the energies and widths of absorption bands are independent of the irradiation dose, and their intensities are proportional to it. No saturation effects are observed in the irradiated samples exposed to a neutron fluence up to 4×10^{17} n/cm^2.

The annealing of the irradiation damage has been shown to be accomplished in two stages. Centers responsible for resonant bands (at photon energies higher than 2.5 eV) recombine through a second-order reaction with an activation energy of 0.3 eV, which is proposed as the activation energy for recombination of close Ga vacancy-interstitial pairs. Centers responsible for extrinsic absorption bands in the range from 1.2 to 2.5 eV disappear through a first-order reaction, with an activation energy of 0.5 eV, which is proposed as the migration energy of Ga vacancies or interstitials.

This model is coherent with the photon energy at which bands are observed and the relative absorption intensity correlation, as both are determined by the vacancy-interstitial distance, through the Coulombian repulsion and the dipole matrix element, respectively.

ACKNOWLEDGMENTS

The authors gratefully acknowledge Dr. Stampfler for the neutron irradiations at the Service de la Pile Universitaire (CRN, Strasbourg). This work has been supported by the project CICYT No. MAT95-0391 of the Spanish Government, and the Projects No. GV-2205/94 and No. GV-3235/95 of Generalitat Valenciana. One of the authors (F.J.M.) wishes to acknowledge the F.P.I. grant from Conselleria d'Educació i Ciència (Generalitat Valenciana).

[1] T. Aono, K. Kase, and A. Kinoshita, J. Appl. Phys. **74**, 2818 (1993).
[2] A. Chevy, J. Appl. Phys. **56**, 978 (1984).
[3] R. Pareja, R. M. de la Cruz, B. Marí, A. Segura, and V. Muñoz, Phys. Rev. B **47**, 2870 (1993).
[4] B. Mari, A. Segura, and A. Chevy, Appl. Surf. Sci. **50**, 415 (1991).
[5] *Handbook of Chemistry and Physics*, 7th ed., edited by R. Weast (CRC, Boca Raton, 1989).
[6] M. A. Vesaghi, Phys. Rev. B **25**, 5436 (1982).
[7] L. A. Miller, D. K. Brice, A. K. Prinja, and S. T. Picraux, in *Defects in Materials*, edited by P. D. Bristow and J. E. Epperson (MRS, Pittsburgh, 1991).
[8] M. Gauthier, A. Polian, J. M. Besson, and A. Chevy, Phys. Rev. B **40**, 3837 (1989).
[9] T. A. McMath and J. C. Irwin Phys. Status Solidi A **38**, 731 (1976).
[10] J. W. Cleland, K. Lark-Horovitz, and C. Pigg, Phys. Rev. **78**, 814 (1950).
[11] J. Bourgoin and M. Lannoo, in *Point Defects in Semiconductors II*, edited by M. Cardona (Springer, Berlin, 1983).
[12] J. Shaffer and F. E. Williams, in *Proceedings of the International Conference on Semiconductor Physics* (Dunod, Paris, 1964), p. 811.
[13] D. G. Thomas, M. Gershenzon, and F. A. Trumbore, Phys. Rev. A **133**, A269 (1964).
[14] F. E. Williams, J. Phys. Chem. Solids **12**, 265 (1960); W. Hoogenstraten, Philips Res. Rep. **13**, 515 (1958).